# Communications

# Electrochemistry at Carbon Nanotube Electrodes: Is the Nanotube Tip More Active Than the Sidewall?**

*Kuanping Gong, Supriya Chakrabarti, and Liming Dai\**

The molecular engineering of an electrode surface is of paramount importance for the development of electrochemical devices with region-specific electron-transfer capabilities. As they have a unique one-dimensional molecular geometry and excellent electronic properties, carbon nanotubes (CNTs) have been widely used as functional electrodes in various electrochemical systems.[1–9] Indeed, carbon nanotubes have been demonstrated to enhance the electrochemical activity of biomolecules[10] and to promote the electron-transfer reactions of redox proteins, such as myoglobin,[11] cyctochrome c,[12] and microperoxidase MP-11.[13] Recent studies[1–4,13–15] have suggested that much of the enhanced electrochemical activity and electron-transfer rate at carbon nanotube electrodes arises from the edge-plane-like nanotube *ends* and that the nanotube *sidewall* is comparable to the basal plane of highly orientated pyrolytic graphite (HOPG). However, no convincing experimental evidence has been obtained owing to technical difficulties in distinguishing the electrochemical role of the nanotube tip from its sidewall, or vice versa, for conventional randomly orientated nanotubes or relatively short aligned nanotubes. This situation was further complicated by oxygen-containing groups, often introduced through chemical/electrochemical oxidation of the CNT tips or sidewalls, which could affect the nanotube electrode kinetics.[15–17] The recent availability of superlong ( ≈5 mm) vertically aligned carbon nanotubes (SLVA-CNTs)[18–21] enabled us to study the electrochemistry of the nanotube tip and sidewall specifically by selectively masking regions of the nanotube with a nonconducting polymer coating (e.g. polystyrene, PS) such that the electrolyte has access the nanotube sidewall or tip only. The effectiveness of the polymer masking was checked by fully coating the nanotube with polystyrene under the same conditions: no electrochemical signal was observed at all. Various electrochemical probes, including $K_3[Fe(CN)_6]$, β-nicotinamide adenine dinucleotide disodium salt hydrate (NADH, reduced form), hydrogen peroxide ($H_2O_2$), oxygen, cysteine, and ascorbic acid (AA) with specific electrochemical sensitivities

to various surface states of an electrode,[22–25] were then used to monitor the electrochemical activities of the nanotube tip and sidewall. Depending on the electrochemical species used, we found that both the nanotube tip and sidewall could play a dominant role in electrochemistry at the carbon nanotube electrode. Furthermore, oxygen-containing surface functionalities induced, for example by electrochemical oxidation, were also demonstrated to regulate electrochemical activities of the carbon nanotube electrode. These new findings reported herein address the longstanding issue concerning the relative roles of the nanotube tip and sidewall to electrochemistry at carbon nanotube electrodes, and should facilitate the design and development of novel CNT-based electrodes of practical significance.

In a typical experiment, SLVA-CNTs (5 mm long) were produced on a $SiO_2$/Si wafer by the water-assisted chemical vapor deposition (CVD) of high-purity (99.99%) ethylene in the presence of an Fe catalyst with helium/$H_2$ (2.5:1 v/v) as a carrier gas under 1 atm pressure at 700°C.[19–21] Figure 1a shows a digital photograph of the as-synthesized SLVA-CNT array. The corresponding scanning electron microscope (SEM) image is reproduced in Figure 1b, which shows closely packed well-aligned individual nanotubes. Transmission electron microscopic (TEM) observation of the constituent nanotubes individually dispersed in ethanol clearly reveals a double-walled carbon nanotube (DWNT) with an average outer diameter of 4 nm (Figure 1c).

Figure 1d shows a schematic representation of the procedure for preparing the nanotube electrode from the as-synthesized SLVA-DWNT array. To start with, a small bundle of the superlong CNTs was taken out from the as-synthesized SLVA-DWNTs and connected to a copper wire (Step 1 in Figure 1d) with silver epoxy (see inset in Figure 1d). The CNT electrode with only the nanotube tip exposed (designated as the CNT-T electrode) was then prepared by thoroughly coating the copper-wire-supported CNTs with a PS solution (15 wt% in toluene) and drying at 50°C in air (Step 2 in Figure 1d), followed by partially cutting off the free end of the polymer-wrapped CNTs (Step 3 in Figure 1d). The access of aqueous electrolytes to the innerwall of the wt nanotube can be effectively limited by the hydrophobic nature of the small DWNT.[9] On the other hand, the CNT electrode with only the nanotube sidewall exposed (designated as the CNT-S electrode) was prepared by coating the two ends of the copper-wire-supported CNTs with the PS solution and drying at 50°C in air (Step 4 in Figure 1d). To prepare the corresponding nanotube electrodes with oxygen-containing surface functionalities (designated as O-CNT-T and O-CNT-S), the newly prepared CNT-T and CNT-S electrodes were polarized at 1.8 V in 0.1 M phosphate-buffered

[*] Dr. K. Gong, Dr. S. Chakrabarti, Prof. Dr. L. Dai
Department of Chemical and Materials Engineering and
Department of Chemistry and UDRI
University of Dayton
300 College Park, Dayton, OH 45469 (USA)
Fax: (+1) 937-229-3433
E-mail: ldai@udayton.edu
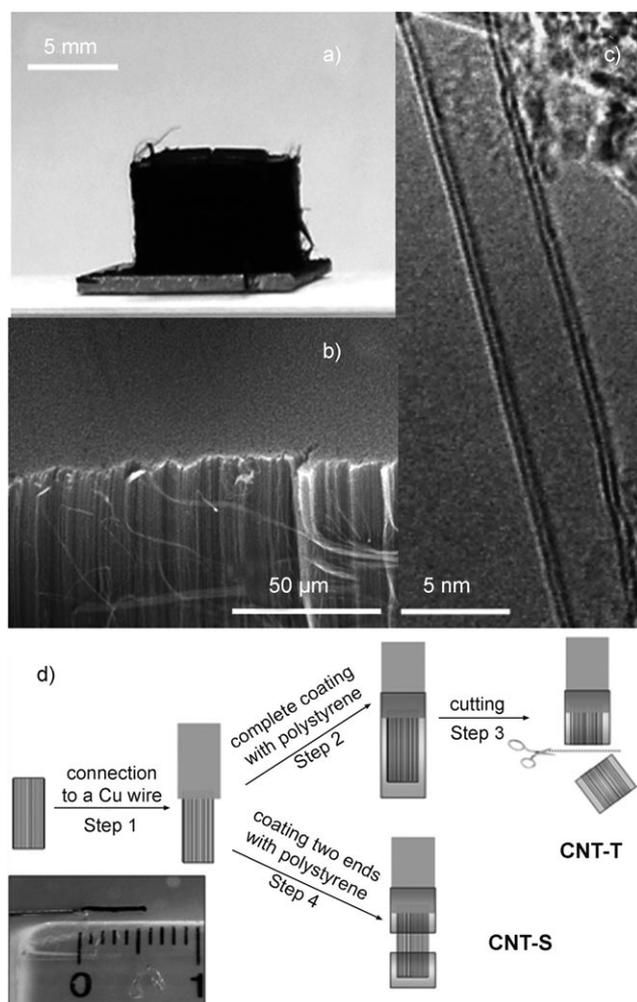
**Figure 1.** a) A digital photograph, b) SEM image, and c) TEM image of the as-synthesized aligned superlong CNTs. d) A schematic representation of the procedure for preparing the CNT electrodes with only the nanotube tip (CNT-T) or sidewall (CNT-S) accessible to electrolyte. The inset in (d) shows a digital photograph of a nanotube electrode thus prepared with an aligned superlong CNT bundle connected to a copper wire.



**Figure 2.** a) Cyclic voltammograms of 5 mM $K_3[Fe(CN)_6]$ recorded in 0.1 M PBS (pH 6.5) at a scan rate of 100 mV s$^{-1}$ for the CNT-T (upper dotted curve), O-CNT-T (upper solid curve), CNT-S (lower dotted curve), and the O-CNT-S electrodes (lower solid curve). For clarification, the current responses at the CNT-T and CNT-S electrodes were amplified and the amplification coefficients are also shown. b) Cyclic voltammograms of 5 mM $K_3[Fe(CN)_6]$ recorded at the O-CNT-T electrode in 0.1 M PBS (pH 6.5) at scan rates of 10, 20, 50, 100, 200, 300, 400 to 500 mV s$^{-1}$ (from inner to outer). Inset in (b) shows the plot of peak current as a function of the square root of the scan rate.

saline solution (PBS, pH 6.5) for 3 min; they were then treated by cycling potential scanning in 0.5 M $H_2SO_4$ until a stable cyclic voltammogram (CV) was recorded.

After the confirmation of the successful electrochemical oxidation by Raman and X-ray photoelectron spectroscopic (XPS) measurements (Figure S1 and S2 in the Supporting Information), these newly prepared and well-characterized CNT-S and CNT-T electrodes with and without the electrochemical oxidation were then used for subsequent electrochemical measurements. Figure 2 shows the cyclic voltammograms of 5 mM potassium ferricyanide ($K_3[Fe(CN)_6]$) at the four different CNT electrodes (i.e. CNT-T, O-CNT-T, CNT-S, O-CNT-S). As can be seen in Figure 2a (lower curves), the electrochemical oxidation did not cause any change in the peak-to-peak separation (i.e. $\Delta E_p \approx 80$ mV) for the CNT-S electrode, indicating that the electron-transfer kinetics is insensitive to the oxygen-containing species on the nanotube sidewall. This is consistent with the observation by McCreery

et al.[23] at glassy carbon electrodes, where the redox couple of $[Fe(CN)_6]^{4-/3-}$ was found to proceed with an outer-sphere mode. In addition, this value of 80 mV is much lower than that of the HOPG base plane with and without electrochemical activation,[3] suggesting a faster electron-transfer rate for the CNT-S electrode. In contrast, different $\Delta E_p$ values were observed for the oxidized (60 mV) and unoxidized (75 mV) CNT-T electrodes under the same conditions (upper curves in Figure 2a). The observed decrease in $\Delta E_p$ by 15 mV indicates an enhanced electron-transfer rate for the oxidized CNT-T electrode, as is the case for the conventional acid-oxidized CNT-modified electrodes.[15–17] Furthermore, the $\Delta E_p$ for the electrochemically oxidized CNT-T electrode is close to 59 mV over the whole range of scan rates from 10 up to 500 mV s$^{-1}$ (Figure 2b); this indicates an almost ideal Nernst system with diffusion control (inset in Figure 2b).[23] The overall smaller values of $\Delta E_p$ observed for the CNT-T and O-CNT-T electrodes with respect to the CNT-S and O-CNT-S electrodes imply much faster electron-transfer kinetics at the nanotube tips in this particular case. This is because the electron transfer at carbon nanotube electrodes could be better facilitated by the edge-plane-like nanotube ends than by the nanotube sidewall, as previously suggested (vide supra).[1,3,17] Furthermore, the perpendicularly aligned carbon nanotube arrays, in which all the nanotube top-ends are on one plane at the interface between the electrode and electrolyte solution, should provide additional advantages for the tip-bound oxygen-containing functionalities to collectively adsorb the electrochemical probe molecules and/or to increase their hydration degree for an enhanced electron-transfer rate at the O-CNT-T electrode (vide supra). The observed relatively high redox current of $K_3[Fe(CN)_6]$ at the CNT-T electrode (upper dotted curve in Figure 2a) with respect to the CNT-S electrode (lower dotted curve in Figure 2a) could be explained by the limited access of the electrolyte to the sidewall of individual nanotubes inside the CNT bundle.

These results are the first experimental evidence for enhanced electrochemical activities at the nanotube tips, as had been suggested by previous publications.[3,14–17] As we

shall see later, however, our further studies on other electrochemical probes indicate that the relative electroactivity of the nanotube tip and sidewall at different oxidation states varies with different electrochemical probes.

Sensitivity to oxidation state but not carbon position: Figure 3a,b show typical voltammograms of 2.0 mM NADH
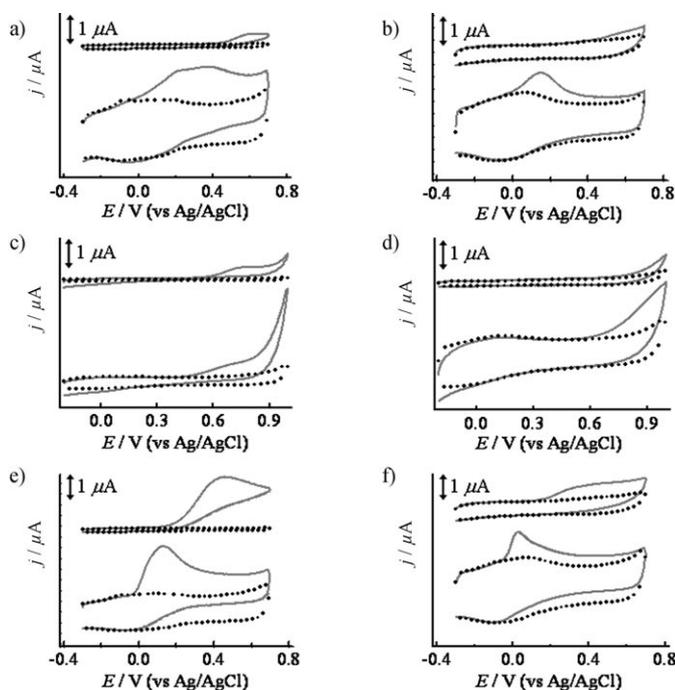


**Figure 3.** Cyclic voltammograms of 2.0 mM NADH (a and b), 2.0 mM H$_2$O$_2$ (c and d), and 2.0 mM ascorbic acid (e and f) recorded in phosphate buffer solution (PBS, pH 6.5) at the CNT-S (upper curves in a, c, and e), O-CNT-S (lower curves in a, c, and e), CNT-T (upper curves in b, d, and f), and O-CNT-T electrodes (lower curves in b, d, and f). The dotted curves were recorded at the corresponding CNT electrodes in the absence of the electrochemical probe molecule. Scan rate: 100 mVs$^{-1}$.

in 0.1M PBS electrolyte (pH 6.5) at the four different CNT electrodes. As can be seen, the CNT-T and CNT-S electrodes (upper curves) have similar oxidation peak potentials ($E_{p,a}$); the same is true for the O-CNT-T and O-CNT-S electrodes (lower curves). However, distinctive peak shifts of about $-0.42$ and $-0.45$ V were observed for the O-CNT-S and O-CNT-T electrodes, respectively, with respect to their unoxidized counterparts. These observations imply that the electrochemical oxidation of NADH is highly sensitive to the presence of oxygen-containing species at both the nanotube tip and sidewall, but not to the basal or edge plane of carbon atoms. For the two oxidized CNT electrodes in pure 0.1M PBS electrolyte (lower dotted curves), a well-defined redox peak was observed at the potential of around 0.0 V arising from the oxygen-containing surface groups induced by the electrochemical oxidation (vide supra). It was further

found that the anodic peak current of the oxygen-containing groups increased whilst the corresponding cathodic peak current decreased upon the stepwise addition of NADH. Therefore, the oxygen-containing groups such as quinine (see Figure S2c in the Supporting Information) introduced by the electrochemical oxidation could act as electron mediators for the NADH oxidation, probably through an electrochemical–chemical–electrochemical mechanism described earlier.[26,27] Electrochemical behavior as similar to that of NADH oxidation was observed for the oxidation of cysteine at the CNT electrodes (see Figure S3 in the Supporting Information).

Sensitivity to carbon position but not oxidation state: Figure 3c,d show the typical voltammograms of 2.0 mM H$_2$O$_2$ in 0.1M PBS electrolyte (pH 6.5) at the four different CNT electrodes. The observed taillike response without any well-defined peak for the CNT-T and O-CNT-T electrodes (Figure 3d) suggests a slow electron-transfer process at the CNT tips. In contrast, a distinctive anodic peak with the formal potential of 0.65 V was clearly observed for both the CNT-S and O-CNT-S electrodes (Figure 3c), indicating a rapid electron-transfer rate with the nanotube sidewall. The H$_2$O$_2$ oxidation is thus sensitive to the presence of edge/basal carbon atoms but not so much to the oxygen-containing functionalities on the CNT electrodes. More interestingly, the electrochemical kinetics for H$_2$O$_2$ oxidation was found in this study to be more favorable at the nanotube sidewall than at its end-tip, in contradiction to earlier reports on some other electrochemical probes.[10,13–15]

Sensitivity to both carbon position and oxidation state: Figure 3e,f show the typical voltammograms of 2.0 mM ascorbic acid (AA) in 0.1M PBS electrolyte (pH 6.5) at the four different CNT electrodes. The observed very different $E_{p,a}$ values for the AA oxidation suggest that the electron-transfer rate in this particular case varies significantly with the presence of not only oxygen-containing groups but also the edge/basal carbon atoms along the CNT structure. The electron transfer was found to be the most favorable at the oxidized tip (i.e. O-CNT-T electrode, lower curves in Figure 3) and least favourable at the unoxidized sidewall (i.e. CNT-S electrode, upper curves in Figure 3e). Similar electrochemical behavior as that for AA was observed for the reduction of oxygen at the CNT electrodes (see Figure S4 in the Supporting Information).

All the numerical results obtained in this study are tabulated in Table 1. The possible deformation of voltammograms (e.g. a decrease in the peak current, an increase in the peak width, and a peak potential displacement depending on the peak current) induced by the ohmic potential drop when

**Table 1:** Summary of the oxidation and reduction peak potentials.[a]

| | $E_{p,a}$ [V] (vs Ag/AgCl) | | | | $E_{p,c}$ [V] (vs Ag/AgCl) | $E_{p,a}-E_{p,c}$ [mV] |
|---|---|---|---|---|---|---|
| | NADH | Cys | H$_2$O$_2$ | AA | Oxygen | Fe(CN)$_6^{4-/3-}$ |
| CNT-S | 0.60 | N[b] | 0.65 | 0.45 | N[b] | 80 |
| O-CNT-S | 0.18[c] | 0.55 | 0.65 | 0.13 | $-0.70$ | 80 |
| CNT-T | 0.60 | N[b] | N[b] | 0.35 | N[b] | 75 |
| O-CNT-T | 0.15 | 0.45 | N[b] | 0.03 | $-0.48$ | 60 |

[a] NADH: dihydronicotinamide adenine dinucleotide; AA: ascorbic acid; Cys: Cysteine. [b] N: No obvious peak. [c] The first peak potential for the oxidation of NADH.

electrode materials were mixed with one or more non-conductive components[28,29] were found to be neglectable in the present study (Figure S5 in the Supporting Information). Further experiments are needed in order to fully understand the governing principle(s) for the influence of the CNT tip/sidewall and its oxidation states on the electron-transfer rate of various electrochemical probes, including those used in this study, at the CNT electrodes. Given that the redox couple of $H_2O_2/H_2O$ proceeds by a two-electron reduction pathway with one water molecule involved in neutral to alkaline media, the unique spin and/or charge distribution along the CNT sidewall[30,31] could significantly enhance the chemisorption of $H_2O_2$ at the CNT sidewall with respect to its tube end, and hence explain the observed substantially increased electrokinetics for the CNT sidewall electrodes in this particular case. On the other hand, McCreery et al.[23] suggested that the AA oxidation at carbon electrodes is an inner-sphere reaction with electron-transfer kinetics highly sensitive to the electrode surface, such as the electronic properties and surface functional groups. In the present study, therefore, the AA oxidation was seen to be sensitive to both the edge or base-plane carbon atoms and the oxidation states of the CNT surface. Unlike the oxidation of NADH at the O-CNT electrodes, however, the observed sensitivity of AA oxidation to the oxidized CNT electrodes could not be attributed to an electron-mediated process associated with the oxygen-containing surface groups since the addition of AA into the pure 0.1M PBS electrolyte did not cause any change in the redox peak currents of the oxygen-containing surface groups.

In summary, we have demonstrated experimentally the effects of the nanotube tip and sidewall, and their oxidation states on the electrochemistry of various commonly used electrochemical probes, including $K_3[Fe(CN)_6]$, NADH, cysteine, $H_2O_2$, oxygen and ascorbic acid, at CNT electrodes. By using superlong ($\approx 5$ mm) vertically aligned carbon nanotube bundles selectively masked with a nonconducting polymer coating at the nanotube sidewall or tip(s), we have successfully limited the electrolyte access to the nanotube tip or sidewall only for region-specific electron transfer between the electrochemical probes and the CNT electrodes. In contradiction to the common belief we found that the electrochemistry at carbon nanotube electrodes is not always facilitated by the nanotube tip and/or oxygen-containing surface groups. In fact, the relative electrosensitivity to the nanotube tip and sidewall and their oxidation states varies with different electrochemical probes (see Table 1) and relates to distinct reaction mechanisms. These new findings address the long-standing issue concerning the role of the nanotube tip or sidewall to electrochemistry at carbon nanotube electrodes, and hence could facilitate the design and development of novel CNT-based electrodes for various potential applications, ranging from electrochemical sensors and biosensors to energy-conversion devices.

## Experimental Section

Chemicals and materials: Potassium ferricyanide ($K_3[Fe(CN)_6]$), hydrogen peroxide ($H_2O_2$, 30%), β-nicotinamide adenine dinucleo-tide disodium salt hydrate (NADH, reduced form), ascorbic acid, and cysteine were purchased from Sigma and used as received. All chemicals were analytical grade and were used without further purification. Aqueous solutions were prepared with doubly distilled water. The SLVA-CNTs (5 mm long) were produced on a $SiO_2/Si$ wafer from Fe catalyst by the water-assisted CVD of high-purity (99.99%) ethylene using helium/$H_2$ (2.5:1 v/v) as a carrier gas under 1 atm pressure at 700°C.[21] Details of the nanotube electrode preparation are described in the text and the preparation procedure is shown in Figure 1d.

Characteriztion: Scanning electron microscopy (SEM) imaging was performed on a Hitachi S-4800 high-resolution SEM unit, whilst transmission electron microscopy (TEM) images were recorded on a Hitachi H-7600 TEM unit. X-ray photoelectron spectroscopic (XPS) measurements were made on a VG Microtech ESCA 2000 using monochromatic $Mg_{K\alpha}$ radiation at a power of 300 W. Raman spectra were obtained using an inVia micro-Raman spectrometer (Renishaw) with an Ar ion laser at a wavelength of 514.5 nm.

Electrochemical measurements were carried out using a computer-controlled potentiostat (CHI 760C, Austin, USA) with a three-electrode configuration. The as-prepared CNT-S, O-CNT-S, CNT-T, or O-CNT-T electrode was used as working electrode and a Pt wire as counterelectrode. All potentials used were biased versus Ag/AgCl electrode (filled with 4.0M KCl). Unless stated otherwise, all electrochemical experiments were performed in air at room temperature (25°C).

[1] J. J. Gooding, *Electrochim. Acta* **2005**, *50*, 3049.
[2] G. G. Wildgoose, C. E. Banks, R. G. Compton, *Small* **2006**, *2*, 182.
[3] C. E. Banks, T. J. Davies, G. G. Wildgoose, R. G. Compton, *Chem. Commun.* **2005**, 829.
[4] J. Wang, *Electroanalysis* **2005**, *17*, 7.
[5] Q. Zhao, Z. Gan, Q. Zhuang, *Electroanalysis* **2002**, *14*, 1609.
[6] M. Gao, S. Huang, L. Dai, G. Wallace, R. Gao, Z. Wang, *Angew. Chem.* **2000**, *112*, 3810; *Angew. Chem. Int. Ed.* **2000**, *39*, 3664.
[7] P. He, L. Dai, *Chem. Commun.* **2004**, 348.
[8] M. Gao, L. Dai, G. Wallace, *Electroanalysis* **2003**, *15*, 1089.
[9] *Carbon Nanotechnology: Recent Developments in Chemistry, Physics, Materials Science and Device Applications* (Ed.: L. Dai), Elsevier: Amsterdam, **2006**.
[10] M. Valcárcel, B. Simonet, S. Cardenas, B. Suarez, *Anal. Bioanal. Chem.* **2005**, *382*, 1783.
[11] C. Zhao, L. Zhang, X. Wei, Z. Yang, *Electrochem. Commun.* **2003**, *5*, 825.
[12] J. Wang, M. Li, L. Shi, N. Li, Z. Gu, *Anal. Chem.* **2002**, *74*, 1993.
[13] J. J. Gooding, R. Wibowo, J. Liu, W. Yang, D. Losic, S. Orbons, F. J. Mearns, J. G. Shapter, D. B. Hibbert, *J. Am. Chem. Soc.* **2003**, *125*, 9006.
[14] A. Chou, T. Böcking, N. K. Singh, J. J. Gooding, *Chem. Commun.* **2005**, 842.
[15] K. Gong, X. Zhu, R. Zhao, S. Xiong, L. Mao, C. Chen, *Anal. Chem.* **2005**, *77*, 8158.
[16] K. Gong, Y. Dong, S. Xiong, Y. Chen, L. Mao, *Biosens. Bioelectron.* **2004**, *20*, 253.
[17] C. G. Banks, R. R. Moore, T. J. Davies, R. G. Compton, *Chem. Commun.* **2004**, 1804.
[18] K. Hata, D. N. Futaba, K. Mizuno, T. Namai, M. Yumura, S. Iijima, *Science* **2004**, *306*, 1362.

[19] S. Chakrabarti, H. Kume, L. Pan, T. Nagasaka, Y. Nakayama, *J. Phys. Chem. C* **2007**, *111*, 1929.

[20] S. Chakrabarti, T. Nagasaka, Y. Yoshikawa, L. Pan, Y. J. Nakayama, *Jpn. J. Appl. Phys. Part 2* **2007**, *45*, L720.

[21] S. Chakrabarti, K. Gong, L. Dai, *J. Phys. Chem. C* **2008**, *112*, 8136.

[22] P. Chen, R. L. McCreery, *Anal. Chem.* **1996**, *68*, 3958.

[23] R. L. McCreery, *In Electroanalytical Chemistry, Vol. 17* (Ed.: A. J. Bard), Dekker, New York, **1991**, pp. 221–374.

[24] M. R. Deakin, K. J. Stutts, R. M. Wightman, *J. Electroanal. Chem.* **1985**, *182*, 113.

[25] F. A. Armstrong, A. M. Bond, H. A. O. Hill, B. N. Olive, I. S. M. Psalti, *J. Am. Chem. Soc.* **1989**, *111*, 9185.

[26] H. Jaegfeldt, A. B. Torstensson, L. Gorton, G. Johansson, *Anal. Chem.* **1981**, *53*, 1979.

[27] A. A. Karyakin, Y. N. Ivanova, K. V. Revunova, E. E. Karyakina, *Anal. Chem.* **2004**, *76*, 2004.

[28] J. Navarro-Laboulais, J. Vilaplana, J. López, J. J. García-Jareño, D. Benito, F. Vicente, *J. Electroanal. Chem.* **2000**, *484*, 33.

[29] D. O'Hare, J. V. Macpherson, A. Willows, *Electrochem. Commun.* **2002**, *4*, 245.

[30] S. Irle, A. Mews, K. Morokuma, *J. Phys. Chem. A* **2002**, *106*, 11973.

[31] T. Kar, B. Akdim, X. Duan, R. Pachter, *Chem. Phys. Lett.* **2004**, *392*, 176.